UDC 551.511.32:532.526/.527

NOTE ON FINITE-DIFFERENCE APPROXIMATIONS FOR THE VISCOUS GENERATION OF VORTICITY AT A BOUNDARY

R. C. BEARDSLEY

Department of Meteorology, Massachusetts Institute of Technology, Cambridge, Mass.

ABSTRACT

The viscous decay of a fluid in solid body rotation in a circular two-dimensional container is studied using a vorticity finite-difference scheme. A comparison is made with the well-known analytic solution to determine the accuracy of several finite-difference expressions for the wall vorticity. The most accurate results are obtained with a first-order scheme that conserves the net integrated vorticity.

1. INTRODUCTION

Consider axisymmetric two-dimensional motion in a circle of unit radius. The fluid is in an initial state of solid body rotation; the azimuthal velocity $v(r,\ t=0)=r$ for $(r<1)$. The tangential velocity must always vanish on the circular boundary, so $v(1,\ t)=0$ for all time.

The mathematical problem of describing the viscous decay of this initial state has a simple analytic solution that allows the accuracy of any numerical integration scheme to be checked directly. Since the ensuing decay is due entirely to the retarding torque generated at the boundary, this problem is well suited to test different finite-difference expressions for the torque or vorticity generated at the wall.

There are other physical systems, of course, that possess analytic solutions; these could be used for such a comparison study. Laminar flow along a pipe or linearized Ekman-layer flow are particularly good examples; the existence of a nontrivial steady-state solution would eliminate the complication of time-differencing errors. We chose the present system, however, because it also models in the simplest nontrivial way "spin up," a class of physical problems currently being studied in geophysical fluid dynamics. In this initial value problem, the angular velocity of a rapidly rotating closed container is suddenly changed by a slight amount. The enclosed fluid, initially conserving its angular momentum, takes on an instantaneous velocity field that decays with increasing time but always satisfies the no-slip condition on the container boundary. A homogeneous fluid adjusts to the new angular velocity through vortex stretching by Ekman layers. For a heavily stratified fluid, the principal adjustment process is the horizontal viscous diffusion of vorticity. The simple system outlined here crudely models this latter case, so the study tests the general applicability of such finite difference schemes to this particular type of initial value problem. Since all calculations will exhibit the same time-differencing errors, a comparison of results for different wall-torque expressions will test their accuracy.

Our problem may be formulated directly in terms of the azimuthal velocity v or in terms of the vertical component of vorticity $\zeta = (1/r)(rv)_r$. We chose the latter approach since (1) the vorticity stream-function formulation is widely used in two-dimensional studies of nondivergent flow and (2) it allows us to evaluate directly the finite-difference expression for the wall torque developed by Bryan (1963) and Pearson (1965). Since by Kelvin's circulation theorem the net vorticity for the continuous system is always zero, a third expression for the viscously generated wall torque is developed on the constraint that net vorticity be conserved.

2. FORMULATION OF THE PROBLEM

The viscous decay of two-dimensional circular motion is governed by the diffusion of vorticity

$$\zeta_t=\nu\nabla^2\zeta \tag{1}$$

where ν is the kinematic viscosity and the vorticity ζ and azimuthal velocity v are defined in terms of a stream function ψ by

$$\zeta=\nabla^2\psi \tag{2}$$

and

$$v=\psi_r. \tag{3}$$

At $t=0$, the fluid is in solid body rotation except at the wall $(r=1)$ where the azimuthal velocity must always vanish to satisfy the no-slip condition.

The analytic expressions for ζ and ψ are given in Bessel function series (Batchelor 1967) by

$$\zeta=-2\sum_{n=1}^{\infty}\frac{J_0(\lambda_n r)}{J_0(\lambda_n)}\,e^{-\lambda_n^2\nu t}$$

and

$$\psi=2\sum_{n=1}^{\infty}\left\{\frac{J_0(\lambda_n r)-J_0(\lambda_n)}{\lambda_n^2 J_0(\lambda_n)}\right\}e^{-\lambda_n^2\nu t}$$

where λ_n is the nth zero of the J_1 Bessel function.

3. CONSERVATION OF NET VORTICITY

The net vorticity when integrated over an area A inside a contour C is by Stokes's theorem the circulation of that contour:

$$\int_A \boldsymbol{\zeta}\cdot d\mathbf{A}=\oint_C \mathbf{u}\cdot d\mathbf{s}. \tag{4}$$

If the contour C coincides with a stationary fluid boundary where the tangential velocity is required to vanish, $\mathbf{u}\cdot d\mathbf{s}$ is identically zero everywhere on the contour. Thus, if the entire fluid boundary is stationary, application of the no-slip condition on the boundary imposes on the vorticity field the kinematic constraint that the integrated or net vorticity must be zero.

4. DEVELOPMENT OF THE FINITE-DIFFERENCE SCHEME

Let Δr and Δt be increments of r and t where $\Delta r=1/J$, J being the number of radial grid points. The grid net is then defined by

$$r_j=j\Delta r, \quad j=0, 1, \ldots, J$$

and

$$t_n=n\Delta t, \quad n=0, 1, 2, \ldots .$$

The finite-difference analog to eq (1) utilizes a forward-difference operator for the time derivative and a center-difference scheme for the Laplacian:

$$\frac{\zeta_j^{n+1}-\zeta_j^n}{\Delta t}=\nu(\nabla^2\zeta^n)_j. \tag{5}$$

The continuous one-dimensional Laplacian operator may be integrated over a small annular shaped area to give the approximation

$$2\pi\int_{r_1}^{r_2}(\nabla^2 f)r dr=2\pi\{(\nabla f\cdot r)_{r_2}-(\nabla f\cdot r)_{r_1}\}$$
$$\simeq\pi(r_2^2-r_1^2)[\nabla^2 f(r=(r_1+r_2)/2)].$$

Choosing $r_1=\Delta r[j-(1/2)]$ and $r_2=\Delta r[j+(1/2)]$ (except at the origin where $r_1=0$) yields for the finite-difference Laplacian (∇^2)

$$(\nabla^2 f)_j=\frac{4}{\Delta r^2}(f_1-f_0), \quad j=0$$

$$=\frac{1}{\Delta r^2}\{A_{+j}f_{j+1}+A_{-j}f_{j-1}-2f_j\}, \quad j>0 \tag{6}$$

where

$$A_{\pm j}=1\pm\frac{1}{2j}.$$

Equation (5) may be integrated systematically in time at all interior points ($j<J$) provided the vorticity generated at the wall is known for each time step. Let us consider the computational sequence of the integration cycle to clarify the role of the wall vorticity in the vorticity-stream function approach.

If we assume that the entire vorticity distribution is known at the nth time step, eq (5) yields the new vorticity field ζ^{n+1} at all interior points ($j<J$). The one-dimensional Poisson problem for ψ^{n+1}, namely that of finding a stream function ψ such that

$$(\nabla^2\psi^{n+1})_j=\zeta_j^{n+1}, \quad j<J \tag{7}$$

subject to $\psi_J=0$, is next solved using one of several techniques (relaxation, Gaussian elimination, etc.). Then an expression of the form

$$\zeta_J^{n+1}=F(\psi_j^{n+1}) \tag{8}$$

is used to obtain an estimate of the wall vorticity. This completes the entire vorticity determination for the $(n+1)$th time step, and the cycle can be initiated again.

The function F is usually determined by a Taylor series expansion of ψ at the boundary where the no-slip condition requires that the normal derivative of ψ vanish. Two such expressions, of first- and second-order accuracy in Δr, respectively, were introduced by Bryan (1963) and Pearson (1965):

$$\zeta_J=\frac{2\psi_{J-1}}{\Delta r^2}, \quad \text{(Bryan)} \tag{9}$$

and

$$\zeta_J=\frac{8\psi_{J-1}-\psi_{J-2}}{2\Delta r^2}, \quad \text{(Pearson)}. \tag{10}$$

As previously discussed, the no-slip condition applied on an entire stationary fluid boundary requires the net vorticity to be zero. A second order finite-difference version of this constraint (4) is

$$\int_A\zeta\cdot d\mathbf{A}\simeq\sum_{j=0}^{J}\zeta_j\Delta A_j=0 \tag{11}$$

where

$$\Delta A_j=\begin{cases}\dfrac{\pi\Delta r^2}{4}, & j=0,\\ 2\pi\Delta r^2 j, & 0<j<J,\\ \pi\Delta r^2\left(J-\dfrac{1}{4}\right), & j=J,\end{cases}$$

each elemental area (excluding the origin and boundary wall) being an annular shaped region of radial thickness Δr centered on a mean radius $j\Delta r$. This approximation (11) is also consistent with the choice of area increments used in the derivation of the finite-difference Laplacian ∇^2.

For determining if a finite-difference scheme is conservative, that is, satisfies eq (11), we perform a summation with the vorticity given by eq (7) at the interior points ($j<J$) and by the expression (8) relating the wall vorticity to the local values of ψ. The scheme is then conservative if the sum equals zero. While neither Bryan's nor Pearson's expressions satisfy this constraint, a form that does conserve net vorticity is easily found:

$$\zeta_J=\left(\frac{2J-1}{J-\frac{1}{4}}\right)\frac{\psi_{J-1}}{\Delta r^2} \quad \text{(conservative)}. \tag{12}$$

It should be noted that Bryan's expression coupled with the usual center-difference form of the divergence operator for a Cartesian grid with equal increments does satisfy the Cartesian version of eq (11).

Computations were made using eq (5) and the three wall-vorticity expressions (9), (10), and (12) for 20- and 40-point radial grids. While the prediction equation is linear with nonconstant coefficients, the von Neumann stability criterion is

$$G=\frac{\nu\Delta t}{\Delta r^2}\leq\frac{1}{4}.$$

The Gaussian elimination procedure (Richtmeyer and Morton 1967) was used to obtain an exact solution of eq (7) for the stream function.

The initial fields used to start the calculations for all schemes were

$$\psi_j^0\,(t=0)=\frac{1}{2}\left(\frac{j^2}{J^2}-1\right),\quad j\leq J,$$

$$\zeta_j^0=2,\quad j<J,$$

and

$$\zeta_J^0=-\frac{2(2J-1)^2}{4J-1}. \tag{13}$$

The wall value ζ_J was computed using the conservative form (12), so that the initial field satisfied the finite-difference form of the integral constraint (11). We felt this procedure particularly relevant since the viscous sidewall boundary layer is initially much thinner than the grid spacing Δr. This problem of adequate boundary-layer resolution is confined to the initial few time steps since the boundary layer thickens quickly with time.

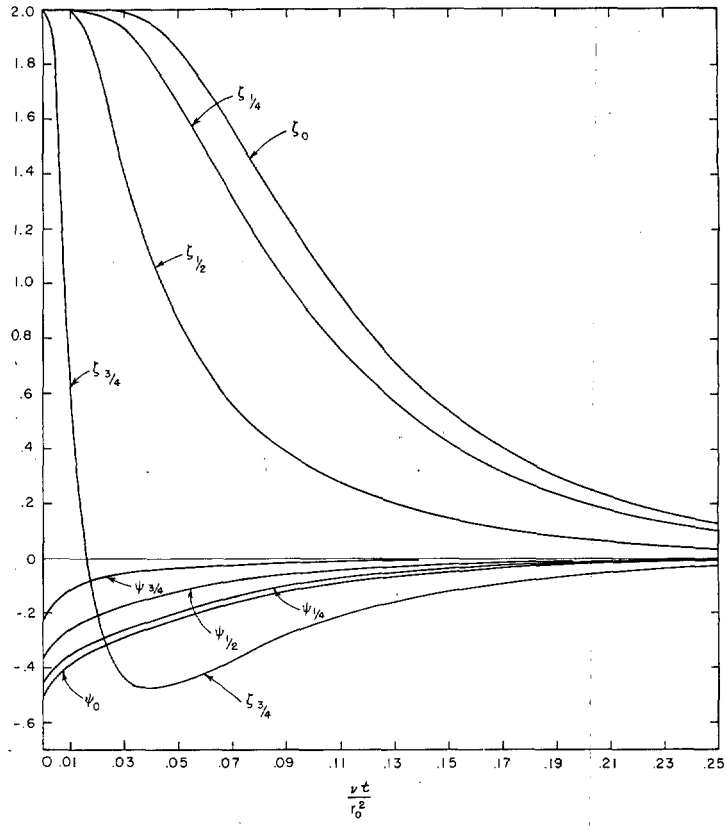

FIGURE 1.—Analytic solution for vorticity ζ and stream function ψ at selected radii.

5. COMPARISON OF ANALYTIC AND NUMERICAL SOLUTIONS

Numerical calculations were performed for 20- and 40-point grids using two stability factors, $G=2/9$ and $1/9$. The numerical vorticity and stream function fields were compared with the analytic solutions at five different radii ($r=0$, 0.25, 0.50, 0.75, 1.0) to determine the overall accuracy of the various numerical schemes. Since both ζ and ψ decay to zero with time and the differences between solutions are relatively small, the comparisons between numerical and analytic use a fractional deviation of the general form

$$D\phi=\frac{\phi(t)_{analytic}-\phi(t)_{numerical}}{\phi(t)_{analytic}}.$$

This expression shows the instantaneous difference between the two solutions at the same point in space normalized by the value of the analytic field at that time. The analytic solutions for ζ and ψ at the comparison radii are shown for reference in figure 1. In the figures that follow, the time coordinate is measured in units of nondimensional time while the letters B, P, and C represent Bryan's first-order, Pearson's second-order, and the conservative expressions, respectively. The values in parentheses following the letters indicate the number of grid points J used in that particular calculation.

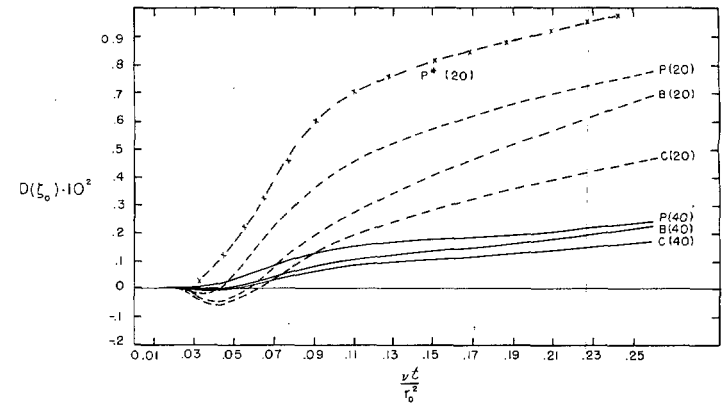

FIGURE 2.—Fractional deviation of vorticity at the center of the circle versus time for $G=2/9$.

We will discuss first and in detail the results for the larger stability factor $G=2/9$. The computed vorticity fields show at all comparison radii that an increase in the spatial resolution for a constant stability factor reduces the magnitude of the fractional error. Since the analytic and numerical solutions for ζ at the center are equal at $t=0^+$, the fractional error $D\zeta$ in figure 2 is initially 0 for all schemes. Then after a short initial period of vorticity overestimation, primarily for the $J=20$ case, all numerical schemes underestimate at the center. The

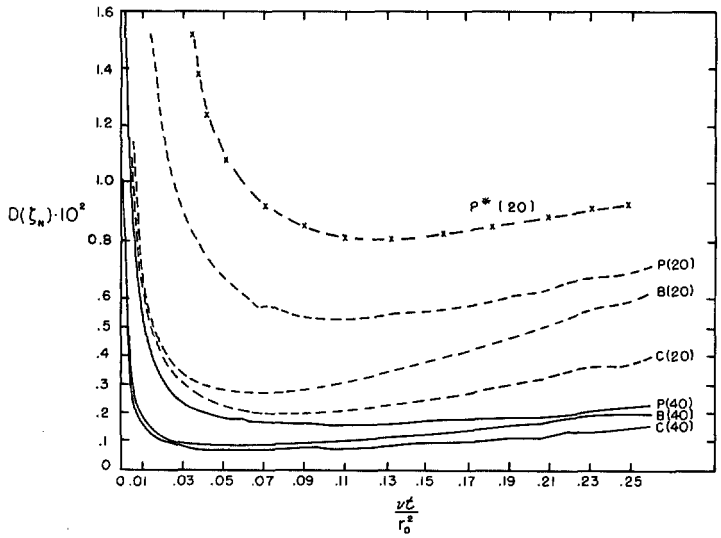

FIGURE 3.—Fractional deviation of vorticity generated at the boundary versus time for $G=2/9$.

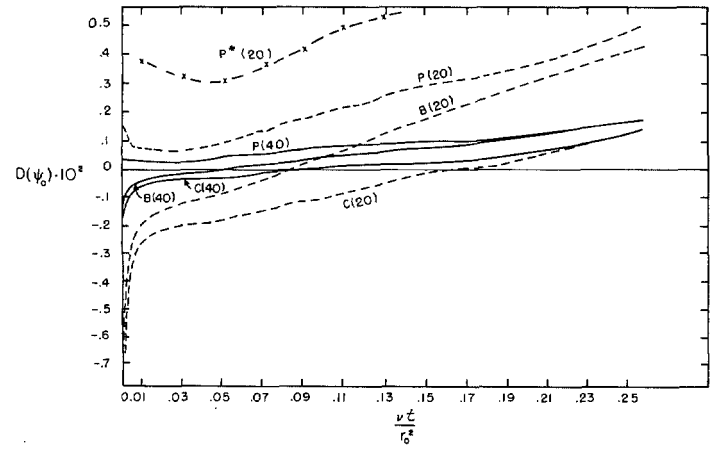

FIGURE 4.—Fractional deviation of stream function at the center of the circle versus time for $G=2/9$.

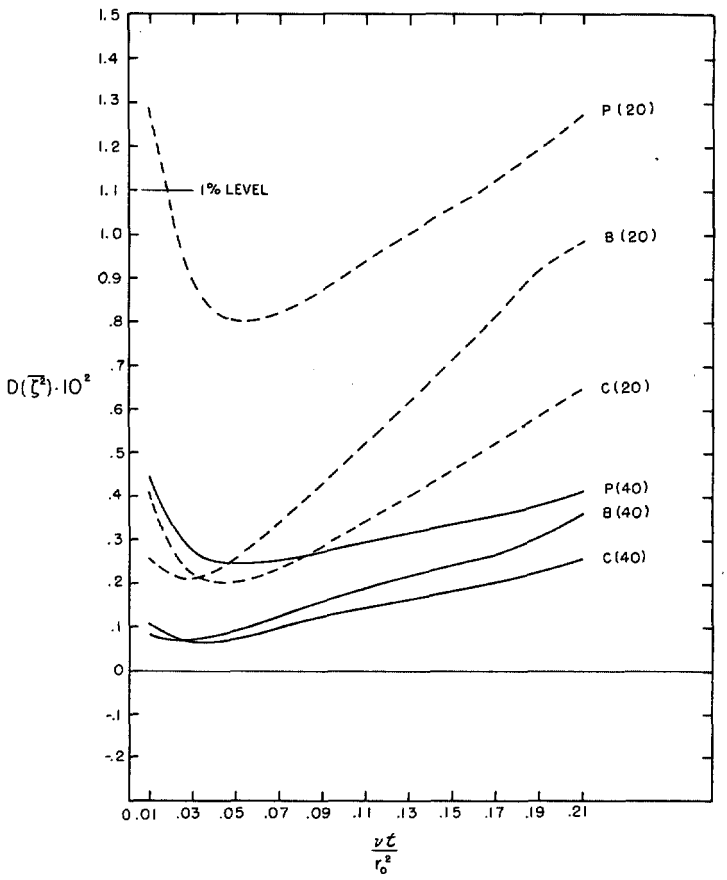

FIGURE 5.—Fractional deviation of $\overline{\zeta}^2$ versus time for $G=2/9$.

behavior of the numerical solutions at the other interior points is similar, with initial overestimation for both $J=20$ and 40 cases occurring at $r=0.5$ and 0.75. While the amount of this initial overestimation increases slightly with increasing radius, the degree of underestimation for larger time (shown in fig. 2) is approximately constant with increasing radius, the conservative scheme showing the minimum deviation.

Part of the overestimation and underestimation of the vorticity field with time is caused by time-differencing errors. The fractional truncation error associated with the forward-difference approximation for the time derivative is $0(\zeta_{tt}\Delta t/\zeta_t)$. We see from figure 1 that while for $t>0$ and $r\leq 0.5$, ζ_{tt} changes sign from negative to positive with increasing time, so that an initial period of overestimation is expected.

While this transient behavior is observed at all interior points, figure 3 shows that the three stream-function expressions for the retarding torque generated at the wall always underestimate the wall vorticity. Although the conservative scheme yields the most accurate prediction, all schemes give reasonably good results. All curves in figure 3 have an initial ordinate of 100 at $t=0^+$since the instantaneous analytic wall torque is ∞ while all numerical solutions remain finite at $t=0^+$. This large starting error, due to the initially poor resolution of the growing viscous boundary layer, decreases as the resolution improves with time. This result suggests that, in other transient problems (especially the spin-up problem), the the initial lack of boundary-layer resolution should not cause appreciable error in either the boundary-layer phenomena or the interior flow with increasing time.

The stream function found directly from the predicted vorticity field also shows underestimation and overestimation at the interior comparison radii. The stream function deviation at the center shown in figure 4 is characteristic of the error patterns exhibited at other radii. Both the Bryan and conservative schemes tend to cause initial overestimation while the second-order schemes of Pearson always underestimate ψ. All schemes show an increased accuracy as the spatial resolution is improved while the conservative scheme appears better only for larger time.

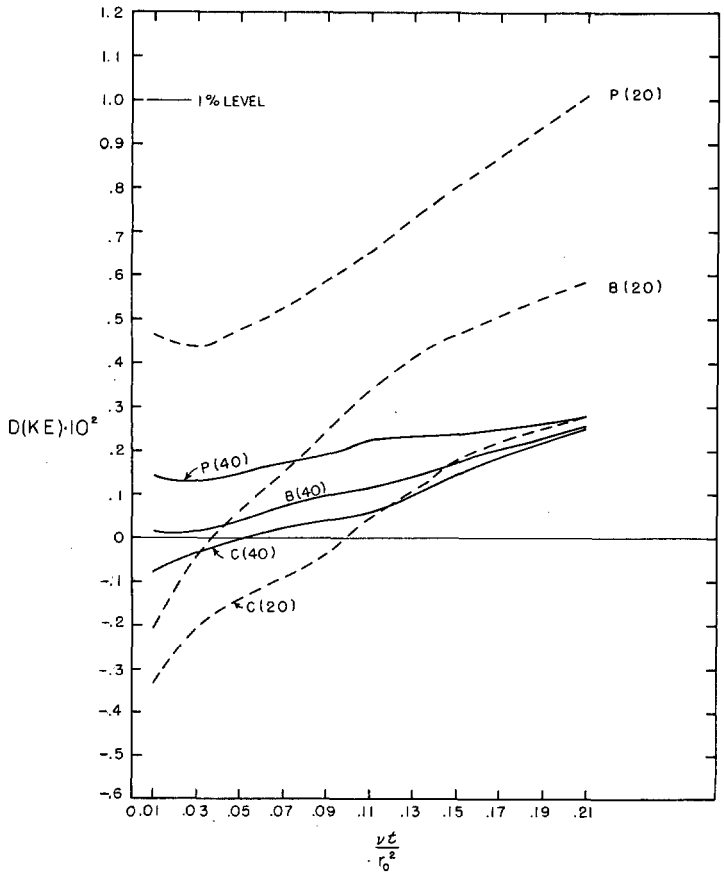

FIGURE 6.—Fractional deviation of kinetic energy (KE) versus time for $G=2/9$.

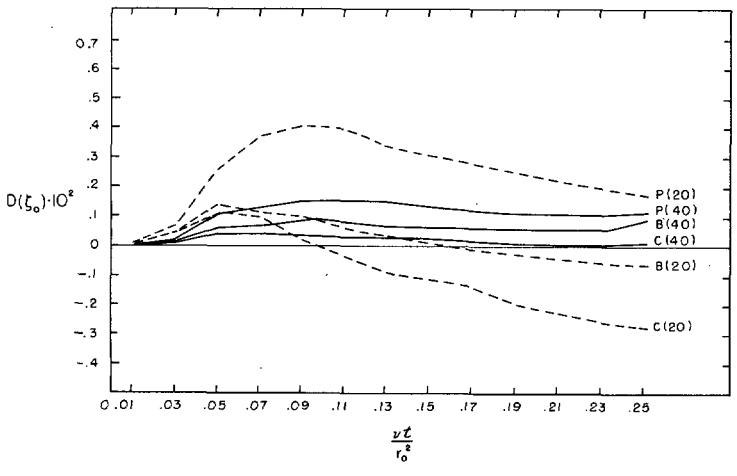

FIGURE 7.—Fractional deviation of vorticity at the center of the circle versus time for the smaller time step, $G=1/9$.

This examination of vorticity and stream-function fields indicates that both Bryan's first-order and the conservative schemes are slightly more accurate than Pearson's higher order scheme. It should be remembered that the conservative expression (12) was used to compute the boundary value for the initial vorticity distribution

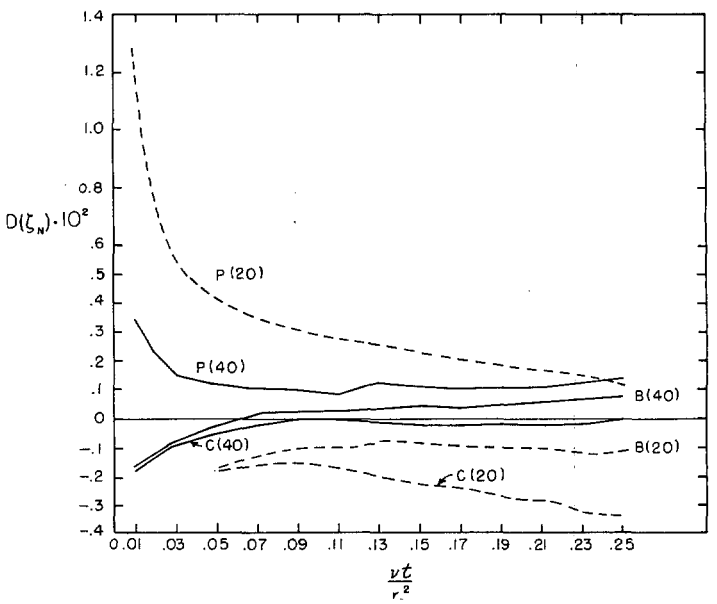

FIGURE 8.—Fractional deviation of boundary vorticity versus time for $G=1/9$.

used to start all numerical integrations, for reasons discussed in the previous section. As a check on this procedure, a calculation was repeated for the 20-point grid using a modified initial vorticity field in which the value of ζ at the boundary was computed from ψ_0 using Pearson's expression (10). The results, shown in figures 2, 3, and 4 for $r=0$ and 1.0 with the label P*, indicate significantly larger errors than those obtained with the original field.

The numerical schemes being tested differ only in boundary conditions on the vorticity field at the wall where the entire retarding torque is generated. Integral properties of the flow like the kinetic energy and mean square vorticity were computed for the numerical solutions using the summation approximation given in eq (11) for the area integral. All three numerical schemes underestimate the mean square vorticity shown in figure 5 while the kinetic energy shown in figure 6 exhibits some intial overestimation. Since the kinetic energy decays more rapidly to zero with time, round-off errors become significant in figure 6 for $\nu t/r_0^2 \geq 0.15$.

The numerical results for the smaller stability factor ($G=1/9$) show several differences from those of the larger stability factor. An increase in the spatial resolution decreases the magnitude of the fractional errors of both ζ and ψ fields, but the numerical schemes now overestimate ζ near the center (see fig. 7) only for large time. This general trend is also illustrated in the wall vorticity results shown in figure 8. The fractional errors in the integrated vorticity-squared and kinetic energy results are shown in figures 9 and 10 for $G=1/9$. Both indicate that after some initial adjustment, the numerical solutions tend to decay slightly more slowly, whereas the kinetic energy and ζ^2 integrals decay more rapidly for the larger

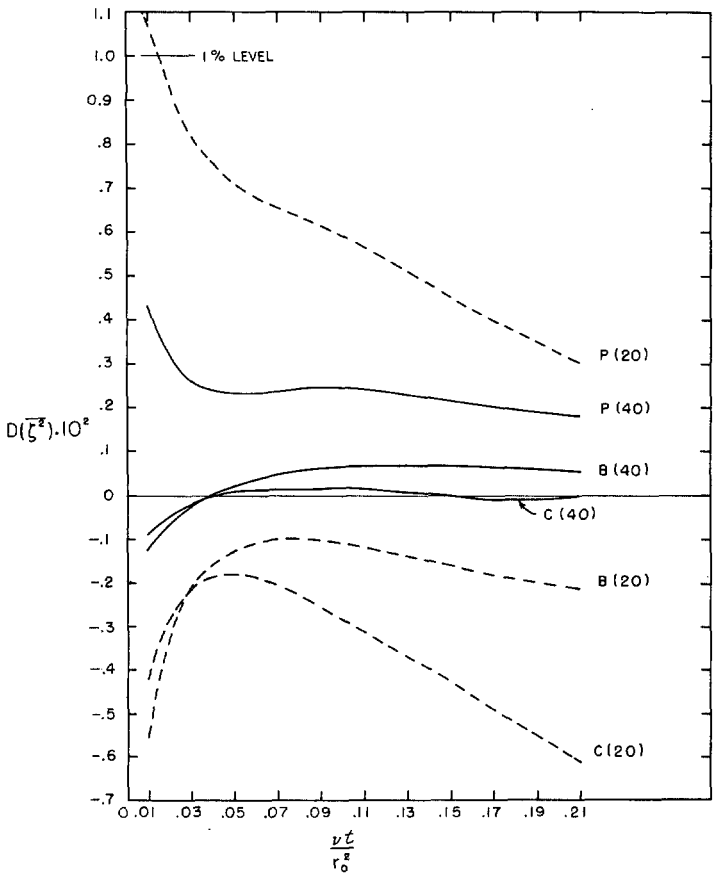

FIGURE 9.—Fractional deviation of $\overline{\zeta^2}$ versus time for $G=1/9$.

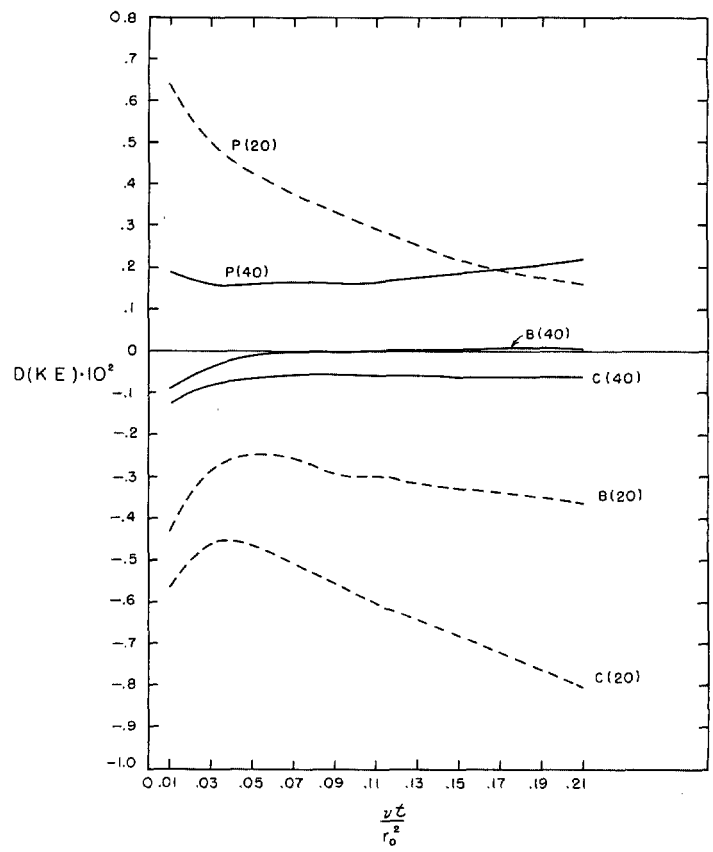

FIGURE 10.—Fractional deviation of kinetic energy (KE) versus time for $G=1/9$.

stability factor. Again, round-off errors become significant in figure 10 for $\nu t/r_0^2 \geq 0.15$. Thus, after the large initial errors, all three schemes give reasonably accurate results with the selection of a "best," that is, most accurate numerical scheme, now noticeably less clear than for the larger stability factor.

6. CONCLUSIONS

The two-dimensional viscous spin-down of a fluid in initial solid body rotation has been studied numerically using both a first-order (Bryan) and second-order (Pearson) expression for the retarding torque generated at the fluid boundary. A third finite-difference expression has been developed that conserves total vorticity. While all schemes tested give reasonably accurate results, the conservative scheme provides the best vorticity prediction resulting in the smallest fractional deviation when the time step is chosen close to the maximum value allowed by the von Neumann stability criteria. However, the choice of the best prediction scheme for smaller time steps is not at all clear. All calculations are noticeably improved by an increase in spatial resolution while only the vorticity values are slightly improved by a decrease in the time step. Over the time range studied, accounting for over-99.9-percent decay in the kinetic energy, the maximum fraction deviation in ζ and $\overline{\zeta^2}$ shown by all three schemes is less than 0.8 percent and 1.4 percent, respectively, after the large initial error due to inadequate boundary-layer resolution has vanished.

ACKNOWLEDGMENTS

I would like to thank N. Phillips for pointing out the net circulation constraint, J. Festa who helped with the coding, and a referee who suggested several improvements. The calculations were performed on the IBM 360/65 at the MIT (Massachusetts Institute of Technology) Information Processing Center. This work represents MIT GFD (Geophysical Fluid Dynamics) Laboratory Report 69-2 and was supported by the Office of Naval Research, Grant NONR-1841(74).

REFERENCES

Batchelor, G. K., *An Introduction to Fluid Dynamics*, Cambridge University Press, England, **1967**, 615 pp.

Bryan, Kirk, "A Numerical Investigation of a Nonlinear Model of a Wind-Driven Ocean," *Journal of the Atmospheric Sciences*, Vol. 20, No. 6, Nov. **1963**, pp. 594–606.

Pearson, C. E., "A Computational Method for Viscous Flow Problems," *Journal of Fluid Mechanics*, Vol. 21, No. 4, **1965**, pp. 611–622.

Richtmeyer, R. D., and Morton, K. W., *Difference Methods for Initial Value Problems*, John Wiley & Sons, Inc., New York, N.Y., **1967**, 405 pp.

[Received February 27, 1970; revised July 6, 1970]